

Anthropic considerations in nuclear physics

Ulf-G. Meißner

Received: date / Accepted: date

Abstract In this short review, I discuss the sensitivity of the generation of the light and the life-relevant elements like carbon and oxygen under changes of the parameters of the Standard Model pertinent to nuclear physics. Chiral effective field theory allows for a systematic and precise description of the forces between two, three, and four nucleons. In this framework, variations under the light quark masses and the electromagnetic fine structure constant can also be consistently calculated. Combining chiral nuclear effective field theory with Monte Carlo simulations allows to further calculate the properties of nuclei, in particular of the Hoyle state in carbon, that plays a crucial role in the generation of the life-relevant elements in hot, old stars. The dependence of the triple-alpha process on the fundamental constants of Nature is calculated and some implications for our anthropic view of the Universe are discussed.

Keywords Anthropic principle · Nuclear Physics · Effective Field Theory

1 A brief guide through this short review

In this review, I discuss certain fine-tunings in nuclear physics that are relevant to the formation of life-relevant elements in the Big Bang and in stars.

Work supported in part by DFG and NSFC (Sino-German CRC 110), Helmholtz Association (contract VH-VI-417), BMBF (grant 05P12PDFTE), the EU (HadronPhysics3 project), and by LENPIC (DEC-2103/10/M/ST2/00420). Computational resources provided by the Jülich Supercomputing Centre (JSC) at the Forschungszentrum Jülich and by RWTH Aachen.

Ulf-G. Meißner

Helmholtz-Institut für Strahlen- und Kernphysik (Theorie) and Bethe Center for Theoretical Physics, Universität Bonn, D-53155 Bonn, Germany

E-mail: meissner@hiskp.uni-bonn.de

Institute for Advanced Simulation (IAS-4), Institut für Kernphysik (IKP-3), Jülich Center for Hadron Physics, JARA HPC and JARA FAME, Forschungszentrum Jülich, D-52425 Jülich, Germany,

Kavli Institute for Theoretical Physics China, CAS, Beijing, 100190, China

To set the stage, in Sec. 2 I give a brief discussion of the so-called anthropic principle and argue that one can indeed perform physics tests of this rather abstract statement for specific processes like element generation. This can be done with the help of high performance computers that allow us to simulate worlds in which the fundamental parameters underlying nuclear physics take values different from the ones in Nature. In Sec. 3 I define the specific physics problems we want to address, namely how sensitive the generation of the light elements in the Big Bang is to changes in the light quark mass m_q ¹ and also, how robust the resonance condition in the triple alpha process, i.e. the closeness of the so-called Hoyle state to the energy of ${}^4\text{He}+{}^8\text{Be}$, is under variations in m_q and the electromagnetic fine structure constant α_{EM} . The theoretical framework to perform such calculations is laid out in Secs. 4 and 5. First, I briefly discuss how the forces between nucleons can be systematically and accurately derived from the chiral Lagrangian of QCD. Second, I show how combining these forces with computational methods allows for truly *ab initio* calculations of nuclei. In this framework, the decades old problem of computing the so-called Hoyle state, a particular resonance in the spectrum of the ${}^{12}\text{C}$ nucleus, and its properties can be solved. This is a necessary ingredient to tackle the problem of the fine-tuning mentioned before. In Sec. 6, I show how the quark mass dependence of the nuclear forces can be consistently calculated within chiral nuclear effective field theory (EFT). Constraints on such variations can be derived from Big Bang nucleosynthesis, as outlined in Sec. 7. Here, we will encounter the first fine-tuning relevant to life on Earth. This, however, requires also heavier elements like carbon and oxygen. The viability of the generation of these elements under changes in the light quark mass and the fine structure constant is discussed in Sec. 8. I summarize the implications of these findings for the anthropic principle in Sec. 9 and give a short summary and outlook in Sec. 10. I note that much more work has been done on the topics discussed here, for recent works and reviews the reader is referred to Refs. [1,2,3] and the papers quoted therein.

2 The anthropic principle

The Universe we live in is characterized by certain parameters that take specific values so that life on Earth is possible. For example, the age of the Universe must be large enough to allow for the formation of galaxies, stars and planets. On more microscopic scales, certain fundamental parameters of the Standard Model of the strong and electroweak interactions like the light quark masses or the electromagnetic fine structure constant must take values that allow for the formation of neutrons, protons and atomic nuclei. At present, we do not have a viable theory to predict the precise values of these constants, although

¹ Throughout this review, we work in two-flavor QCD with up and down quarks with masses m_u and m_d , respectively. In most cases, it suffices to work in the isospin limit $m_u = m_d \equiv m_q$ but at one instance we also have to consider strong isospin breaking with $m_u \neq m_d$.

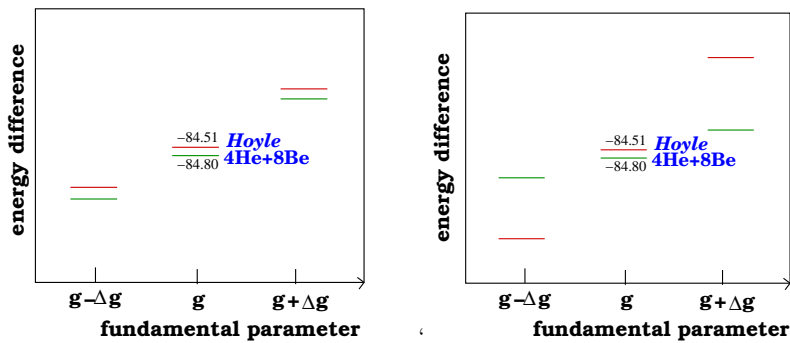


Fig. 1 Resonance condition for carbon production (closeness of the Hoyle state to the ${}^4\text{He}+{}^8\text{Be}$ threshold) in stars as a function of some fundamental parameter g . Left panel: Non-anthropic scenario, right panel: anthropic scenario.

string theory promises to do so in some distant future. Clearly, one can think of many universes, the multiverse, in which various fundamental parameters take different values leading to environments very different from ours. In that sense, our Universe has a preferred status, and this was the basis of the so-called *anthropic principle* (AP) invented by Carter [4]. The AP states that “the observed values of all physical and cosmological quantities are not equally probable but they take on values restricted by the requirement that there exist sites where carbon-based life can evolve and by the requirements that the Universe be old enough for it to have already done so”. There are many variants of the AP, but this definition serves our purpose quite well. At first sight, one might think that it is a tautology, as the statement seems to be a tautology. However, we can move away from the philosophical level and ask whether the AP can have physical consequences that can be tested? This is indeed the case particularly in nuclear physics, as I will argue in this review. But it is worth mentioning that anthropic reasoning has been used in some well cited papers, I name here Weinberg’s work on the cosmological constant [5] and Susskind’s exploration of the string theory landscape [6]. The influence of the AP on string theory and particle physics has been reviewed recently in Ref. [3]. But let us return to nuclear physics. A prime example of the AP is the so-called Hoyle state. In 1954, Hoyle [7] made the prediction of an excited level in carbon-12 to allow for a sufficient production of heavy elements (${}^{12}\text{C}$, ${}^{16}\text{O}$,...) in stars. As the Hoyle state is crucial to the formation of the elements essential to life as we know it, this state has been nicknamed the “level of life” [8]. See, however, Ref. [9] for a thorough historical discussion of the Hoyle state in view of the anthropic principle. Independent of these historical issues, the anthropic view of the Universe can be nicely shown using the example of the Hoyle state, more precisely, one can understand how the abstract principle can be turned into a physics question. The central issue is the closeness of the Hoyle state to the threshold of ${}^4\text{He}+{}^8\text{Be}$ that determines the resonance enhancement of carbon production. In Fig. 1 I show the possible response of

this resonance condition to the change of some fundamental parameter, here called g . If for a wide range of this parameter, the resonance condition stays intact (left panel), more precisely, the absolute energies might shift but the Hoyle state stays close to the energy of ${}^4\text{He}+{}^8\text{Be}$. In such a case, one can hardly speak of an anthropic selection. If on the other hand, the two levels split markedly for small changes in g as shown in the right panel, this would correspond to a truly anthropic fine-tuning. In Nature, we can not investigate which of these scenarios is indeed fulfilled as all fundamental constants take specific values. However, with the powerful tool of computer simulations this has become possible and this issue will be discussed in the remaining part of the review.

3 Definition of the physics problem

In this section, I will more precisely define the nuclear physics problems that have implications for our anthropic or non-anthropocentric view of the Universe. As it is well known, the elements that are pertinent to life on Earth are generated in the Big Bang and in stars through the fusion of protons, neutrons and nuclei. In Big Bang nucleosynthesis (BBN), alpha particles (${}^4\text{He}$ nuclei) and some other light elements are generated. Life essential elements like ${}^{12}\text{C}$ and ${}^{16}\text{O}$ are generated in hot, old stars, where the so-called triple-alpha reaction plays an important role. Here, two alphas fuse to produce the unstable, but long-lived ${}^8\text{Be}$ nucleus. As the density of ${}^4\text{He}$ nuclei in such stars is high, a third alpha fuses with this nucleus before it decays. However, to generate a sufficient amount of ${}^{12}\text{C}$, an excited state in ${}^{12}\text{C}$ at an excitation energy of 7.65 MeV with spin zero and positive parity is required [7], this is the famous Hoyle state (for a recent review on the Hoyle state, see Ref. [10]). In a further step, carbon is turned into oxygen without such a resonant condition. So we are faced with a multitude of fine-tunings which need to be explained. We know that all strongly interacting composites like hadrons and nuclei must emerge from the underlying gauge theory of the strong interactions, Quantum Chromodynamics (QCD), that is formulated in terms of quarks and gluons. These fundamental matter and force fields are, however, confined. Note that the mass of the light quarks relevant for nuclear physics is very small ($m_u \simeq 2$ MeV and $m_d \simeq 4$ MeV in the $\overline{\text{MS}}$ scheme at $\mu = 2$ GeV) and thus plays little role in the total mass of nucleons and nuclei. However, the light quark masses are of the same size as the binding energy per nucleon. Further, the formation of nuclei from neutrons and protons requires the inclusion of electromagnetism, characterized by the fine-structure constant $\alpha_{\text{EM}} \simeq 1/137$. So the question we want to address in the following is: How sensitive are these strongly interacting composites to variations in the fundamental parameters of the Standard Model? or stated differently: how accidental is life on Earth?

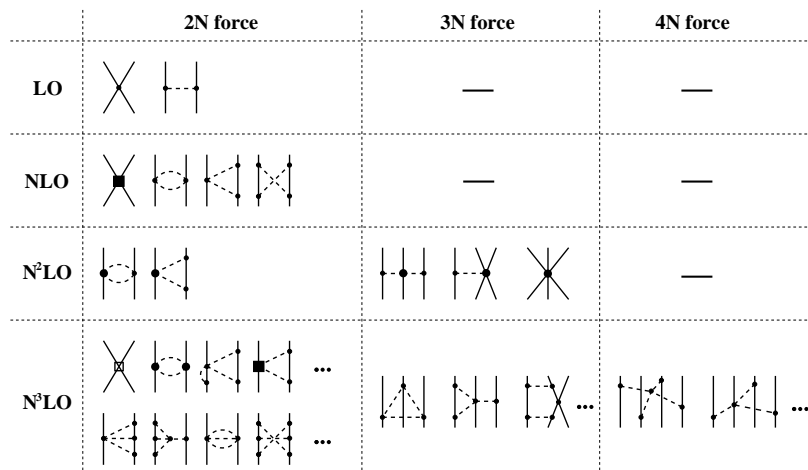


Fig. 2 Contributions to the effective potential of the 2N, 3N and 4N forces based on Weinberg's power counting. Here, LO denotes leading order, NLO next-to-leading order and so on. Dimension one, two and three pion-nucleon interactions are denoted by small circles, big circles and filled boxes, respectively. In the 4N contact terms, the filled and open box denote two- and four-derivative operators, respectively.

4 Chiral symmetry and nuclear forces

It is known since long that chiral symmetry plays an important role in a consistent and precise description of the forces between nucleons. However, a truly systematic approach based on the chiral effective Lagrangian of QCD only became available through the groundbreaking work of Weinberg [11]. As realized by Weinberg, the power counting of the underlying EFT does not apply directly to the S-matrix, but rather to the effective potential - these are all diagrams without N -nucleon intermediate states. Such diagrams lead to pinch singularities in the infinite nucleon mass limit (the so-called static limit), so that e.g. the nucleon box graph is enhanced as m_N/Q^2 , with m_N the nucleon mass and Q a small momentum. The power counting formula for the graphs contributing with the ν^{th} power of Q or a pion mass to the effective potential reads (considering only connected pieces):

$$\nu = -2 + 2N + 2L + \sum_i V_i \Delta_i, \quad \Delta_i = d_i + \frac{n_i}{2} - 2. \quad (1)$$

Here, N is the number of in-coming and out-going nucleons, L the number of pion loops, V_i counts the vertices of type i with d_i derivatives and/or pion mass insertions and n_i is the number of nucleons participating in this kind of vertex. Because of chiral symmetry, $\Delta_i \geq 0$, and thus the leading terms contributing e.g. to the two-nucleon potential can easily be identified. These are the time-honored one-pion exchange and two four-nucleon contact interactions without derivatives. They can be derived from the lowest order effective chiral

Lagrangian with $\Delta_i = 0$ as indicated by the superscript '(0)',

$$\begin{aligned} \mathcal{L}^{(0)} = & \frac{1}{2} \partial_\mu \boldsymbol{\pi} \cdot \partial^\mu \boldsymbol{\pi} - \frac{1}{2} M_\pi^2 \boldsymbol{\pi}^2 + N^\dagger \left[i \partial_0 + \frac{g_A}{2F_\pi} \boldsymbol{\tau} \boldsymbol{\sigma} \cdot \boldsymbol{\nabla} \boldsymbol{\pi} - \frac{1}{4F_\pi^2} \boldsymbol{\tau} \cdot (\boldsymbol{\pi} \times \dot{\boldsymbol{\pi}}) \right] N \\ & - \frac{1}{2} C_S (N^\dagger N)(N^\dagger N) - \frac{1}{2} C_T (N^\dagger \boldsymbol{\sigma} N) \cdot (N^\dagger \boldsymbol{\sigma} N) + \dots, \end{aligned} \quad (2)$$

where $\boldsymbol{\pi}$ and N refer to the pion and nucleon field operators, respectively, and $\boldsymbol{\sigma}$ ($\boldsymbol{\tau}$) denote the spin (isospin) Pauli matrices. Further, g_A (F_π) is the nucleon axial coupling (pion decay) constant and $C_{S,T}$ are the LECs accompanying the leading contact operators without derivatives. The ellipses refer to terms involving more pion fields. It is important to emphasize that chiral symmetry leads to highly nontrivial relations between the various coupling constants. For example, the strengths of all $\Delta_i = 0$ -vertices without nucleons with 2, 4, 6, ... pion field operators are given in terms of F_π and M_π . Similarly, all single-nucleon $\Delta_i = 0$ -vertices with 1, 2, 3, ... pion fields are expressed in terms of just two LECs, namely g_A and F_π . The corrections to the potential are then generated from the higher order terms in the Lagrangian. The so-constructed effective potential is iterated in the Schrödinger or Lippman-Schwinger equation, generating the shallow nuclear bound states as well as scattering states. This requires regularization, a topic still under current debate, but I do not want to enter this issue here, see e.g. Ref. [13].

The resulting contributions at various orders to the 2N, the 3N and the 4N forces are depicted in Fig. 2. Remarkably, by now the 2N, 3N and 4N force contributions have been worked out to N³LO, the last missing piece, namely the N³LO corrections to the 3N forces, was only provided recently [14, 15, 16]. Note, however, that the 3N forces might not have fully converged at this order, and therefore a systematic study of N⁴LO contributions is underway by the Bochum group [17, 18]. This EFT approach shares a few advantages over the very well developed and precise semi-phenomenological approaches, just to mention the consistent derivation of 2N, 3N and 4N forces as well as electroweak current operators, the possibility to work out theoretical uncertainties and to improve the precision by going to higher orders and, of course, the direct connection to the spontaneously and explicitly broken chiral symmetry of QCD. There has been a large body of work on testing and developing these forces in few-nucleon systems, for comprehensive reviews see [13, 19]. As an appetizer, I show in Fig. 3 the description of two-nucleon scattering observables, namely the neutron-proton differential cross section and the analyzing power at $E_{\text{lab}} = 50$ MeV, in this type of approach compared to more conventional and less systematic meson-exchange models.

5 Ab initio solution of the nuclear many-body problem

For systems up to four nucleons, one can calculate their properties using the Faddeev-Yakubowsky machinery or using hyperspherical harmonics or other

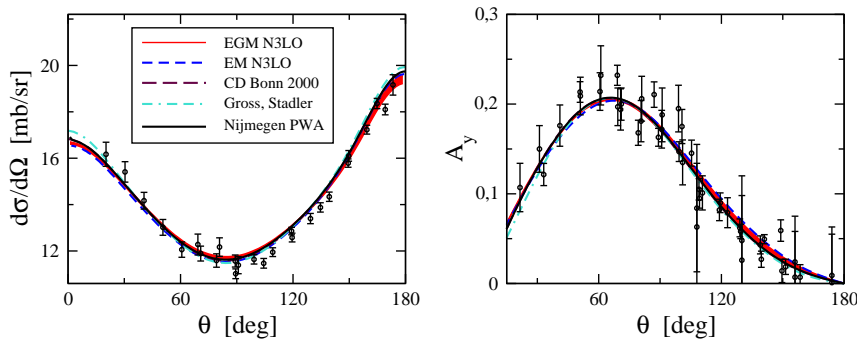


Fig. 3 Neutron-proton differential cross section $d\sigma/d\Omega$ (left panel) and analyzing power A_y (right panel) at $E_{\text{lab}} = 50$ MeV calculated using chiral EFT at $N^3\text{LO}$ by Epelbaum, Glöckle and Meißner (EGM) [20] and Entem and Machleidt (EM) [21], the CD Bonn 2000 potential of Ref. [22] and the potential developed by Gross and Stadler in Ref. [23]. Also shown are results from the Nijmegen partial wave analysis [24]. References to data can be found in [24].

well developed methods. However, since we are interested in carbon and oxygen, we also have to consider the nuclear many-body problem, which refers to nuclei with atomic number $A > 4$. The most modern tool to be used here are the so-called *nuclear lattice simulations*. They combine the power of EFT to generate few-nucleon forces with computational methods to exactly solve the non-relativistic A -body system, where in a nucleus A counts the number of neutrons plus protons. The basic ideas and definitions are spelled out in Ref. [25] and for a detailed review on lattice methods for non-relativistic systems, I refer to Ref. [26]. Here I give only a very short account of this method. The basic idea is to discretize space-time and to introduce a smallest length (the lattice spacing) in the spatial directions and in the temporal direction, denoted a and a_t , respectively. The world is thus mapped onto a finite space-time volume $L \times L \times L \times L_t$ in integer multiples of a and a_t , so $L = Na$ and $L_t = N_t a_t$, respectively. Typical values are $N = 6$ and $N_t = 10 \dots 15$. A Wick rotation to Euclidean space is naturally implied. Note that the finite lattice spacing a entails an ultra-violet (UV) cutoff (a maximal momentum), $p_{\text{max}} = \pi/a$. In typical simulations of atomic nuclei, one has $a \simeq 2$ fm and thus $p_{\text{max}} \simeq 300$ MeV. In contrast to lattice QCD, the continuum limit $a \rightarrow 0$ is not taken. This formulation allows to calculate the correlation function

$$Z(t) = \langle \psi_A | \exp(-tH) | \psi_A \rangle, \quad (3)$$

where t is the Euclidean time, H the nuclear Hamiltonian constructed along the lines described in Sec. 4 and $|\psi_A\rangle$ an A -nucleon state. Using standard methods, one can derive any observable from the correlation function, e.g. the ground-state energy is simply the infinite time limit of the logarithmic derivative of $Z(t)$ with respect to the time. Similarly, excited states can be generated by starting with an ensemble of standing waves, generating a correlation matrix $Z^{ji}(t) = \langle \psi_A^j | \exp(-tH) | \psi_A^i \rangle$, which upon diagonalization generates the

ground and excited states - the larger the initial state basis, the more excited states can be extracted. The initial states are standing waves, projected onto the proper quantum numbers of spin and parity. From these standing waves, the general wave functions $\psi_j(\mathbf{n})$ ($j = 1, \dots, A$) with well-defined momentum using all possible translations, $L^{-3/2} \sum_{\mathbf{m}} \psi_j(\mathbf{n} + \mathbf{m}) \exp(i\mathbf{P} \cdot \mathbf{m})$, can be constructed. Thus, the center-of-mass problem is taken care of. Another recently developed method is based on more complicated initial position-space wave functions [27]. A proper choice for the ψ_j allows one to prepare certain types of initial states, such as shell-model wave functions, which can be symbolically written as (of course, proper antisymmetrization has to be performed)

$$\psi_j(\mathbf{n}) = \exp[-c\mathbf{n}^2], \quad \psi'_j(\mathbf{n}) = n_x \exp[-c\mathbf{n}^2], \quad \psi''_j(\mathbf{n}) = n_y \exp[-c\mathbf{n}^2], \dots, \quad (4)$$

or, for later use, alpha-cluster wave functions,

$$\psi_j(\mathbf{n}) = \exp[-c(\mathbf{n} - \mathbf{m})^2], \quad \psi'_j(\mathbf{n}) = \exp[-c(\mathbf{n} - \mathbf{m}')^2], \quad \dots, \quad (5)$$

where \mathbf{n} , \mathbf{m} , \dots are triplets of integers that represent a lattice site, and n_x, n_y, \dots the components of these vectors. The possibility to construct all these different types of initial/final states is a reflection of the fact that in the underlying EFT all possible configurations to distribute nucleons over all lattice sites are generated. This includes in particular the configuration where four nucleons are located at one lattice site, so there is no restriction like e.g. in a no-core-shell model approach, in which one encounters serious problems with the phenomenon of clustering, that is so prominent in nuclear physics. It is also important to note that the nuclear forces have an approximate spin-isospin SU(4) symmetry (Wigner symmetry) [28] that is of fundamental importance in suppressing the malicious sign oscillations that plague any Monte Carlo simulation of strongly interacting Fermion systems at finite density. The relation of the Wigner symmetry to the nuclear EFT formulation has been worked out in Ref. [29] and its consequences for lattice simulations are explored in Refs. [30, 31].

As one application of this method, I want to discuss the spectrum of ^{12}C and in particular the Hoyle state. This excited state has been an enigma for nuclear structure theory since decades, even the most successful Greens function MC methods based on realistic two- and three-nucleon forces [32] or the no-core-shell-model employing modern (renormalization group softened chiral) interactions [33,34] have not been able to describe this state. The first *ab initio* calculation of the Hoyle state based on nuclear lattice simulations was reported in Ref. [35]. In the meantime, the calculation of the spectrum and the structure of ^{12}C has been considerably improved, using the aforementioned position-space initial and final state wave functions [27]. The predictions for the even-parity states in the ^{12}C spectrum are collected in Tab. 1. In all cases, the LO calculation is within 10% of the experimental number, and the three-nucleon forces at NNLO are essential to achieve agreement with experiment. We remark, however, that the so-called leading order subsumes various

Table 1 The even-parity spectrum of ^{12}C from nuclear lattice simulations. The ground state is denoted as O_1^+ and the Hoyle state as O_2^+ . The NLO corrections include strong isospin breaking as well as the Coulomb force. The NNLO corrections are generated by the leading three-nucleon forces. The theoretical errors include both Monte Carlo statistical errors and uncertainties due to extrapolation at large Euclidean time.

	0_1^+	2_1^+	0_2^+	2_2^+
LO	-96(2) MeV	-94(2) MeV	-88(2) MeV	-84(2) MeV
NLO	-77(3) MeV	-72(3) MeV	-71(3) MeV	-66(3) MeV
NNLO	-92(3) MeV	-86(3) MeV	-84(3) MeV	-79(3) MeV
Exp.	-92.2 MeV	-87.7 MeV	-84.5 MeV	-82.2(1) MeV [36]

important higher order corrections, since the LO four-nucleon contact interactions are smeared with a Gaussian-type function as discussed in Ref. [25]. The Hoyle state is clearly recovered and comes out at almost the same energy as the $^4\text{He}+^8\text{Be}$ threshold - thus allowing for the resonant enhancement of carbon production that was first considered by Hoyle half a century ago. Furthermore, one finds a second 2^+ excited state that has been much debated in the literature. It agrees with the most recent determinations [36]. It is worth to stress that the method has been improved since the results shown in Tab. 1 have been obtained. The ground state energy of ^{12}C can now be calculated with an accuracy of about 200 keV [37]. As already pointed out, the chiral nuclear EFT will also allow one to investigate how the closeness of the Hoyle state to the $^4\text{He}+^8\text{Be}$ threshold depends on the fundamental parameters like the light quark masses, thus allowing for a test of the anthropic principle. For a first attempt within an alpha-cluster model, see Ref. [38].

So far, nuclear lattice simulations have been performed at NNLO, which includes the leading and dominant three-nucleon force topologies, see Refs. [39, 40]. For nuclei up to carbon-12, this is a good approximation due to the small cut-off $\Lambda = p_{\text{max}} \simeq 300$ MeV, which is a much softer interaction than used in the description of continuum NN scattering. Still, higher orders have eventually to be included to reduce the theoretical uncertainties. Also, going to heavier nuclei one observes some overbinding with these NNLO forces [37] that grows with atomic number A . This also requires the inclusion of higher order corrections to the two- and three-nucleon forces. Work in this direction is under way.

6 The nuclear force at varying quark mass

In the Weinberg approach to the nuclear forces, the quark mass dependence of these forces can be worked out straightforwardly. To be precise, one encounters *explicit* and *implicit* quark mass dependences. While the former are generated through the pion propagator, the latter stem from the quark mass dependence of the pion-nucleon coupling constant $\sim g_A/(2F_\pi)$, the nucleon mass, and the 4N couplings, respectively, see Fig.4. Throughout, we use the Gell-Mann-

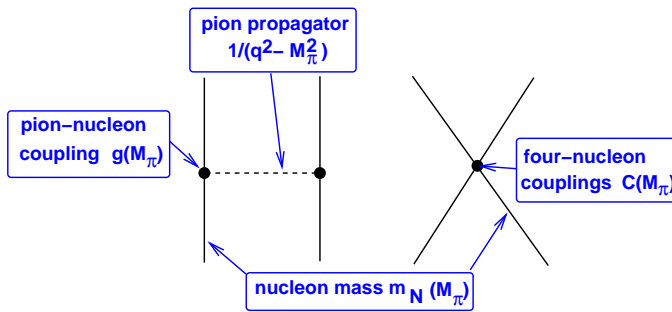


Fig. 4 Explicit and implicit pion (quark) mass dependence of the leading order nucleon-nucleon (NN) potential. Solid (dashed) lines denote nucleons (pions).

Oakes–Renner relation,

$$M_\pi^2 = B(m_u + m_d) + \mathcal{O}((m_u + m_d)^2), \quad (6)$$

with B a low-energy constant related to the scalar quark condensate. In QCD, this relation is fulfilled to about 95% [41], so one can use the wording pion and quark mass dependence synonymously. For any observable \mathcal{O} of a hadron H , we can define its quark mass dependence in terms of the so-called K -factor,

$$\frac{\delta \mathcal{O}_H}{\delta m_f} \equiv K_H^f \frac{\mathcal{O}_H}{m_f}, \quad (7)$$

with $f = u, d$, and m_f the corresponding quark mass. The pion mass dependence of pion and nucleon properties can be obtained from lattice QCD combined with chiral perturbation theory as detailed in Ref. [42]. The pertinent results are:

$$K_{M_\pi}^q = 0.494_{-0.013}^{+0.009}, \quad K_{F_\pi}^q = 0.048 \pm 0.012, \quad K_{m_N}^q = 0.048_{-0.006}^{+0.002}, \quad (8)$$

where q denotes the average light quark mass. To a good approximation, $K_{g_A}^q \simeq 0$. For the quark mass dependence of the short-distance terms, one has to resort to modeling using resonance saturation [43]. This induces a sizeable uncertainty that might be overcome by lattice QCD simulations in the future. For the NN scattering lengths and the deuteron binding energy (BE), this leads to

$$K_{1S0}^q = 2.3_{-1.8}^{+1.9}, \quad K_{3S1}^q = 0.32_{-0.18}^{+0.17}, \quad K_{\text{BE(deut)}}^q = -0.86_{-0.50}^{+0.45}, \quad (9)$$

extending and improving earlier work based on EFTs and models [44, 45, 46, 47, 48]. The running of the NN scattering lengths and the deuteron BE with the light quark mass is shown in Fig. 5. Note, however, that there are recent lattice QCD simulations at large pion masses of about 500 and 800 MeV that seem to indicate a decrease of the deuteron BE with pion mass [49, 50]. How solid extrapolations from such large values down to the physical pion mass are, remains however questionable. In addition to shifts in m_q , we shall also consider the effects of shifts in α_{EM} . The treatment of the Coulomb interaction in the nuclear lattice EFT framework is described in detail in Ref. [51].

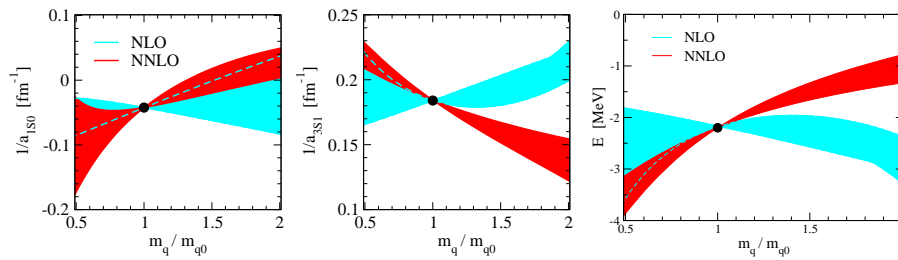


Fig. 5 Quark mass dependence of the inverse scattering length $1/a_{1S0}$ (left panel) and $1/a_{3S1}$ (center panel) and the deuteron binding energy (right panel). Here, m_{q0} denotes the physical light quark mass.

7 Constraints from Big Bang Nucleosynthesis

Using the results from the previous section, one can now analyze what constraints the element abundances in BBN on possible quark mass variations imply. At the beginning, we keep the electromagnetic fine structure constant fixed and work in the isospin limit $m_u = m_d = m_q$. In BBN, elements up to ${}^7\text{Li}$ and ${}^7\text{Be}$ are produced, but in what follows we consider only the variation of the NN scattering lengths, the deuteron BE and we also need the variation of the BEs of ${}^3\text{He}$ and ${}^4\text{He}$ with the pion mass. Following Bedaque, Luu and Platter (for short BLP) [52] these can be obtained by convoluting the 2N K -factors with the variation of the 3- and 4-particle BEs with respect to the singlet and triplet NN scattering lengths. This gives

$$K_{3\text{He}}^q = -0.94 \pm 0.75, \quad K_{3\text{He}}^q = -0.55 \pm 0.42, \quad (10)$$

for details I refer to Ref. [42]. These values are consistent with a direct calculation using nuclear lattice simulations, $K_{3\text{He}}^q = -0.19 \pm 0.25$ and $K_{3\text{He}}^q = -0.16 \pm 0.26$ [53]. With this input, we can calculate the BBN response matrix of the primordial abundances Y_a at fixed baryon-to-photon ratio,

$$\frac{\delta Y_a}{\delta m_q} = \sum_{X_i} \frac{\delta \ln Y_a}{\delta \ln X_i} K_{X_i}^q, \quad (11)$$

with X_i the relevant BEs for ${}^2\text{H}$, ${}^3\text{H}$, ${}^3\text{He}$, ${}^4\text{He}$, ${}^6\text{Li}$, ${}^7\text{Li}$ and ${}^7\text{Be}$ and the singlet NN scattering length, using the updated Kawano code (for details, see Ref. [54]). Comparing the calculated with the observed abundances, one finds that the most stringent limits arise from the deuteron abundance [deut/H] and the ${}^4\text{He}$ abundance normalized to the one of protons, ${}^4\text{He}(Y_p)$, as most neutrons end up in the alpha nucleus. Combining these leads to the constraint $\delta m_q/m_q = (2 \pm 4)\%$. These values are consistent with earlier determinations based on models of the nuclear forces. In contrast to these earlier determinations, we provide reliable error estimates due to the underlying EFT. However, as pointed out by BLP, one can obtain an even stronger bound due to the neutron lifetime, which strongly affects ${}^4\text{He}(Y_p)$. To properly address this

issue, one has of course to include strong isospin violation, as the neutron-proton mass difference receives a 2 MeV contribution from the light quark mass difference and about -0.7 MeV from the electromagnetic interactions. Re-evaluating this constraint under the model-independent assumption that *all* quark and lepton masses vary with the Higgs vacuum expectation value (VEV) v , leads to

$$\left| \frac{\delta v}{v} \right| = \left| \frac{\delta m_q}{m_q} \right| \leq 0.9\% . \quad (12)$$

This is similar to what has been found by BLP, however, they assumed that when m_q changes, m_u/m_d and all other Standard Model parameters stay constant. Such a scenario is hard to reconcile with the Higgs mechanism that gives mass to all fundamental particles $\sim v$ - it would require some very intricate fine-tuning of Yukawa couplings. Constraints on the variations of the Higgs VEV from nuclear binding have also been considered in Ref. [55]. Also, very recently bounds on quark mass and α_{EM} variations from an *ab initio* calculation of the neutron-proton mass difference have been reported [56].

8 The fate of carbon-based life as a function of the fundamental parameters of the Standard Model

I now turn to the central topic of this review, namely how fine-tuned is the production of carbon and oxygen with respect to changes in the fundamental parameters of QCD+QED? Or, stated differently, how much can we detune these parameters from their physical values to still have an habitable Earth as shown in Fig. 6. To be more precise, we must specify which parameters we can vary. In QCD, the strong coupling constant is tied to the nucleon mass through dimensional transmutation. However, the light quark mass (here, only the strong isospin limit is relevant) is an external parameter. Naively, one could argue that due to the small contribution of the quark masses to the proton and the neutron mass, one could allow for sizeable variations. However, the relevant scale to be compared to here is the average binding energy per nucleon, $E/A \leq 8$ MeV (which is much smaller than the nucleon mass). As noted before, the Coulomb repulsion between protons is an important ingredient in nuclear binding, therefore we must also consider changes in α_{EM} . Therefore, in the following we will consider variations in the light quark mass m_q at fixed fine structure constant α_{EM} and also changes in α_{EM} at fixed m_q . The tool to do this are nuclear lattice simulations, which allowed e.g. for the first *ab initio* calculation of the Hoyle state [35].

Let us consider first QCD, i.e. variations in the light quark mass at fixed α_{EM} (for details, see Refs. [57,58]). We want to calculate the variations of the pertinent energy differences in the triple-alpha process $\delta\Delta E/\delta M_\pi$, which according to Fig. 4 boils down to (we consider small variations around the physical value of the pion mass M_π^{ph}):

$$\left. \frac{\partial E_i}{\partial M_\pi} \right|_{M_\pi^{\text{ph}}} = \left. \frac{\partial E_i}{\partial \tilde{M}_\pi} \right|_{M_\pi^{\text{ph}}} + x_1 \left. \frac{\partial E_i}{\partial m_N} \right|_{m_N^{\text{ph}}} + x_2 \left. \frac{\partial E_i}{\partial g_{\pi N}} \right|_{g_{\pi N}^{\text{ph}}}$$

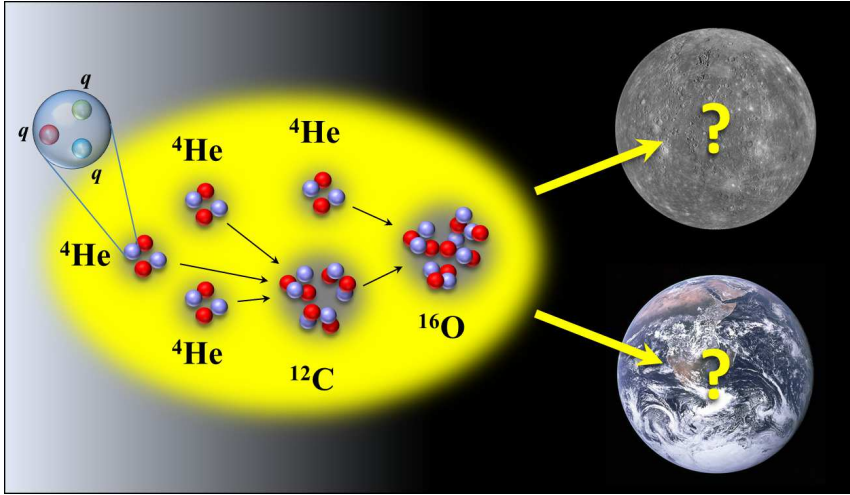


Fig. 6 Graphical representation of the question of how fine-tuned life on Earth is under variations of the average light quark mass and α_{EM} . Figure courtesy of Dean Lee.

$$+ x_3 \left. \frac{\partial E_i}{\partial C_0} \right|_{C_0^{\text{ph}}} + x_4 \left. \frac{\partial E_i}{\partial C_I} \right|_{C_I^{\text{ph}}}, \quad (13)$$

with the definitions

$$x_1 \equiv \left. \frac{\partial m_N}{\partial M_\pi} \right|_{M_\pi^{\text{ph}}}, \quad x_2 \equiv \left. \frac{\partial g_{\pi N}}{\partial M_\pi} \right|_{M_\pi^{\text{ph}}}, \quad x_3 \equiv \left. \frac{\partial C_0}{\partial M_\pi} \right|_{M_\pi^{\text{ph}}}, \quad x_4 \equiv \left. \frac{\partial C_I}{\partial M_\pi} \right|_{M_\pi^{\text{ph}}}, \quad (14)$$

with \tilde{M}_π the pion mass appearing in the pion-exchange potential. The various derivatives in Eq. (13) can be obtained precisely using Auxiliary Field Quantum Monte Carlo (AFQMC) techniques, as examples we show the various contributions to the energy and the various derivatives for ${}^4\text{He}$ and ${}^{12}\text{C}$ in Fig. 7. The x_i ($i = 1, 2, 3, 4$) are related to the pion and nucleon as well as the two-nucleon K -factors determined in Sec. 6. As described in detail in Ref. [58], the current knowledge of the quark mass dependence of the nucleon mass, the pion decay constant and the pion-nucleon coupling constant leads to $x_1 = 0.57 \dots 0.97$ and $x_2 = -0.056 \dots 0.008$ (in lattice units). The scheme-dependent quantities $x_{3,4}$ can be traded for the pion-mass dependence of the inverse singlet a_s and triplet a_t scattering lengths,

$$\bar{A}_s \equiv \left. \frac{\partial a_s^{-1}}{\partial M_\pi} \right|_{M_\pi^{\text{ph}}}, \quad \bar{A}_t \equiv \left. \frac{\partial a_t^{-1}}{\partial M_\pi} \right|_{M_\pi^{\text{ph}}}. \quad (15)$$

We can then express all energy differences appearing in the triple-alpha process

$$\Delta E_b \equiv E_8 - 2E_4, \quad \Delta E_h \equiv E_{12}^* - E_8 - E_4, \quad \varepsilon \equiv E_{12}^* - 3E_4, \quad (16)$$

where E_4 and E_8 denote the energies of the ground states of ${}^4\text{He}$ and ${}^8\text{Be}$, respectively, and E_{12}^* denotes the energy of the Hoyle state, as functions of

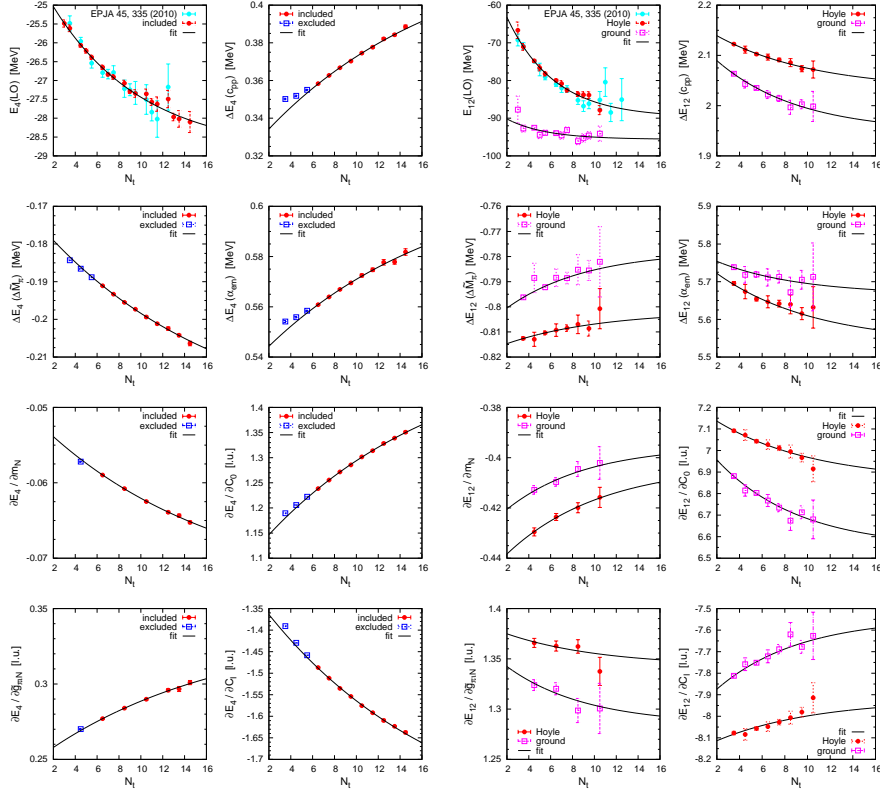


Fig. 7 AFQMC calculation of ${}^4\text{He}$ (left panels) and ${}^{12}\text{C}$ (right panels), as a function of Euclidean time steps N_t . For definition of the various energies and derivatives shown, see Ref. [58]. The results of Ref. [51] for $E_{12}^*(\text{LO})$ are included to highlight the improved statistics, and as a consistency check.

\bar{A}_s and \bar{A}_t . One finds that all these energy differences are correlated, i.e. the various fine-tunings in the triple-alpha process are not independent of each others, see the left panel of Fig. 8. Further, one finds a strong dependence on the variations of the ${}^4\text{He}$ BE, which is strongly suggestive of the α -cluster structure of the ${}^8\text{Be}$, ${}^{12}\text{C}$ and Hoyle states. Such correlations related to the production of carbon have indeed been speculated upon earlier [59,60], but only with the techniques displayed here one could finally derive them from first principles.

Consider now the reaction rate of the triple-alpha process as given by

$$r_{3\alpha} = 3^{\frac{3}{2}} N_\alpha^3 \left(\frac{2\pi\hbar^2}{|E_4|k_B T} \right)^3 \frac{\Gamma_\gamma}{\hbar} \exp\left(-\frac{\varepsilon}{k_B T}\right), \quad (17)$$

with N_α the α -particle number density in the stellar plasma with temperature T , $\Gamma_\gamma = 3.7(5)$ meV the radiative width of the Hoyle state and k_B is Boltz-

mann's constant. The stellar modeling calculations of Refs. [61, 62] suggest that sufficient abundances of both carbon and oxygen can be maintained within an envelope of ± 100 keV around the empirical value of $\varepsilon = 379.47(18)$ keV. This condition can be turned into a constraint on shifts in m_q that reads (for more details, see Ref. [58])

$$\left| \left[0.572(19) \bar{A}_s + 0.933(15) \bar{A}_t - 0.064(6) \right] \left(\frac{\delta m_q}{m_q} \right) \right| < 0.15\% . \quad (18)$$

The resulting constraints on the values of \bar{A}_s and \bar{A}_t compatible with the condition $|\delta\varepsilon| < 100$ keV are visualized in the right panel of Fig. 8. The various shaded bands in this figure cover the values of \bar{A}_s and \bar{A}_t consistent with carbon-oxygen based life, when m_q is varied by 0.5%, 1% and 5%. Given the current theoretical uncertainty in \bar{A}_s and \bar{A}_t , our results remain compatible with a vanishing $\partial\varepsilon/\partial M_\pi$, in other words with a complete lack of fine-tuning. Interestingly, Fig. 8 (right panel) also indicates that the triple-alpha process is unlikely to be fine-tuned to a higher degree than $\simeq 0.8\%$ under variation of m_q . The central values of \bar{A}_s and \bar{A}_t from Ref. [54] suggest that variations in the light quark masses of up to 2 – 3% are unlikely to be catastrophic to the formation of life-essential carbon and oxygen. A similar calculation of the tolerance for shifts in the fine-structure constant α_{EM} proceeds as follows. For small variations $|\delta\alpha_{\text{em}}/\alpha_{\text{em}}| \ll 1$ at the fixed physical value of m_q , the resulting change in ε can be expressed as

$$\delta(\varepsilon) \approx \left. \frac{\partial\varepsilon}{\partial\alpha_{\text{em}}} \right|_{\alpha_{\text{em}}^{\text{ph}}} \delta\alpha_{\text{em}} = Q_{\text{em}}(\varepsilon) \left(\frac{\delta\alpha_{\text{em}}}{\alpha_{\text{em}}} \right) , \quad (19)$$

where $Q_{\text{em}}(\varepsilon) = 3.99(9)$ MeV receives contributions from the long-range Coulomb force and a pp contact term (for details, we refer to Ref. [58]). Recalling further that $K_{M_\pi}^q = 0.494_{-0.013}^{+0.009}$ [42], the condition $|\delta(\varepsilon)| < 100$ keV leads to the predicted tolerance $|\delta\alpha_{\text{em}}/\alpha_{\text{em}}| \simeq 2.5\%$ of carbon-oxygen based life to shifts in α_{em} . This result is compatible with the $\simeq 4\%$ bound reported in Ref. [61].

9 A short discussion of the anthropic principle

Let us pause and discuss the findings obtained in the previous sections. First, it is important to stress that we only consider deformations of the Standard Model that can be expressed through variations of the light quark mass and the electromagnetic fine structure constant. One could imagine a completely different approach to the strong and electroweak interactions that might also lead to carbon-oxygen based life given the proper cosmological conditions. While that is certainly possible, it goes beyond the type of tests we are after. Thus, we will not further consider such possibilities but rather discuss our more modest approach.

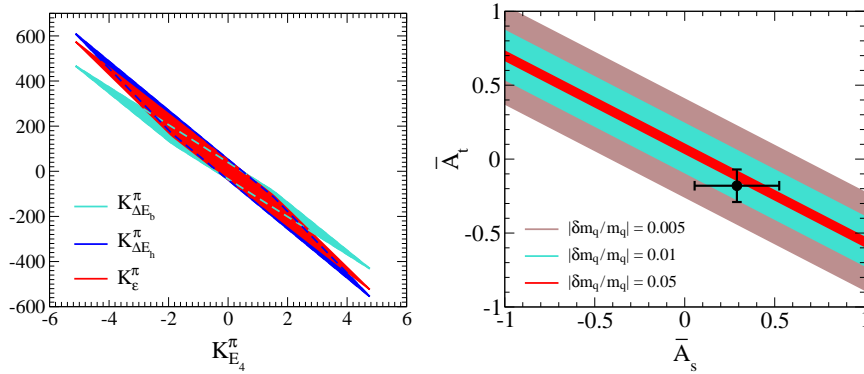


Fig. 8 Left panel: Sensitivities of ΔE_h , ΔE_b and ε to changes in M_π , as a function of $K_{E_4}^\pi$ under independent variation of \bar{A}_s and \bar{A}_t over the range $\{-1 \dots 1\}$. The bands correspond to ΔE_b , ε and ΔE_h in clockwise order. Right panel: “Survivability bands” for carbon-oxygen based life from Eq. (18), due to 0.5% (broad outer band), 1% (medium band) and 5% (narrow inner band) changes in m_q in terms of the input parameters \bar{A}_s and \bar{A}_t . The most up-to-date N²LO analysis of \bar{A}_s and \bar{A}_t from Ref. [54] is given by the data point with horizontal and vertical error bars.

Consider first the element generation in the Big Bang. From the observed element abundances and the fact that the free neutron decays in about 882 s and the surviving neutrons are mostly captured in ^4He , one finds a stringent bound on the light quark mass variations as given in Eq. (12), under the reasonable assumption that the masses of all quarks and leptons appearing in neutron β -decay scale with the Higgs VEV. Thus, BBN sets indeed very tight limits on the variations of the light quark mass. Such extreme fine-tuning supports the anthropic view of our Universe.

The situation concerning the fine-tuning in the triple-alpha process is somewhat less clear. As noted already in Refs. [59,60], the allowed variations in ε (remember that the size of ε defines the resonance condition for carbon production) are not that small, as $|\delta\varepsilon/\varepsilon| \simeq 25\%$ still allows for carbon-oxygen based life. So one might argue that the anthropic principle is indeed *not* needed to explain the fine-tunings in the triple-alpha process. However, as we just showed, this translates into allowed quark mass variations of 2–3% and modifications of the fine-structure constant of about 2.5%. The fine-tuning in the fundamental parameters is thus much more severe than the one in the energy difference ε . Therefore, beyond such relatively small changes in the fundamental parameters, the anthropic principle indeed appears necessary to explain the observed abundances of ^{12}C and ^{16}O . Of course, to sharpen these statements, one must be able to reduce the uncertainty in the determination of the quark mass dependence of the LO four-nucleon contact operators given by the quantities \bar{A}_s and \bar{A}_t . It is hoped that lattice QCD simulations of the two-nucleon system will be able to reduce the sizable uncertainty in these parameters.

10 Summary and outlook

In this short review, I have summarized recent developments in our understanding of the fine-tuning in the generation of the life-essential elements as well as the light elements generated in BBN. As shown, the allowed parameter variations in QCD+QED are small, giving some credit to the anthropic principle. To sharpen these conclusions, future work is required. On one side, lattice QCD at sufficiently small quark masses will eventually be able to give tighter constraints on the parameters $A_{s,t}$ and on the other side, nuclear lattice simulations have to be made more precise to further reduce the theoretical error in the binding and excitation energies and to provide *ab initio* calculations of nuclear reactions, for first steps, see Refs. [63,64]. Finally, we remark that we have considered here QCD with a vanishing θ -angle. For a recent study on variations of θ on the deuteron BE and the triple-alpha process, see Ref. [65].

Acknowledgments

I am grateful to Steve Weinberg, whose query on the resonance condition triggered part of the work done here. I would like to thank my NLEFT collaborators Evgeny Epelbaum, Hermann Krebs, Timo Lähde, Dean Lee and also Gautam Rupak for a most enjoyable collaboration. Some part of this work was done in collaboration with Julian Berengut, Victor Flambaum, Christoph Hanhart, Jenifer Nebreda and Jose Ramon Peláez. I would also like to thank Zhizhong Xing for giving me the opportunity to write this review. I am grateful to Evgeny Epelbaum, Dean Lee and Qiang Zhao for a careful reading of the manuscript.

References

1. R. L. Jaffe, A. Jenkins and I. Kimchi, Phys. Rev. D **79**, 065014 (2009).
2. L. A. Barnes, arXiv:1112.4647 [physics.hist-ph].
3. A. N. Schellekens, Rev. Mod. Phys. **85**, no. 4, 1491 (2013).
4. B. Carter, “Large number coincidences and the anthropic principle”, in *Confrontation of cosmological theories with observational data*, edited by M. S. Longair (Reidel, Dordrecht, 1974).
5. S. Weinberg, Phys. Rev. Lett. **59**, 2607 (1987).
6. L. Susskind, “The Anthropic landscape of string theory,” in *Universe or multiverse?*, edited by B. Carr (Cambridge University Press, Cambridge, England, 2007).
7. F. Hoyle, Astrophys. J. Suppl. Ser. **1**, 121 (1954).
8. A. Linde, “The inflationary multiverse,” in *Universe or multiverse?*, edited by B. Carr (Cambridge University Press, Cambridge, England, 2007).
9. H. Kragh, Arch. Hist. Exact Sci. **64**, 721 (2010).
10. M. Freer and H. O. U. Fynbo, Prog. Part. Nucl. Phys. **78** (2014) 1.
11. S. Weinberg, Phys. Lett. B **251**, 288 (1990).
12. S. Weinberg, Nucl. Phys. B **363**, 3 (1991).
13. E. Epelbaum, H.-W. Hammer, and U.-G. Meißner, Rev. Mod. Phys. **81**, 1773 (2009).
14. S. Ishikawa and M. R. Robilotta, Phys. Rev. C **76**, 014006 (2007).
15. V. Bernard, E. Epelbaum, H. Krebs and U.-G. Meißner, Phys. Rev. C **77**, 064004 (2008).
16. V. Bernard, E. Epelbaum, H. Krebs and U.-G. Meißner, Phys. Rev. C **84**, 054001 (2011).

17. H. Krebs, A. Gasparyan and E. Epelbaum, Phys. Rev. C **85**, 054006 (2012).
18. H. Krebs, A. Gasparyan and E. Epelbaum, Phys. Rev. C **87**, 054007 (2013).
19. R. Machleidt and D. R. Entem, Phys. Rept. **503**, 1 (2011).
20. E. Epelbaum, W. Glöckle and U.-G. Meißner, Nucl. Phys. A **747**, 362 (2005).
21. D. R. Entem and R. Machleidt, Phys. Rev. C **68**, 041001 (2003).
22. R. Machleidt, Phys. Rev. C **63**, 024001 (2001).
23. F. Gross and A. Stadler, Phys. Rev. C **78**, 014005 (2008) [arXiv:0802.1552 [nucl-th]].
24. V. G. J. Stoks, R. A. M. Kompl, M. C. M. Rentmeester and J. J. de Swart, Phys. Rev. C **48**, 792 (1993).
25. B. Borasoy, E. Epelbaum, H. Krebs, D. Lee and U.-G. Meißner, Eur. Phys. J. A **31**, 105 (2007).
26. D. Lee, Prog. Part. Nucl. Phys. **63**, 117 (2009).
27. E. Epelbaum, H. Krebs, T. A. Lähde, D. Lee and U.-G. Meißner, Phys. Rev. Lett. **109**, 252501 (2012).
28. E. Wigner, Phys. Rev. **51**, 106 (1937).
29. T. Mehen, I. W. Stewart, M. B. Wise, Phys. Rev. Lett. **83**, 931 (1999).
30. J. W. Chen, D. Lee and T. Schfer, Phys. Rev. Lett. **93**, 242302 (2004).
31. D. Lee, Phys. Rev. Lett. **98**, 182501 (2007).
32. S. C. Pieper, Riv. Nuovo Cim. **31**, 709 (2008).
33. P. Navratil, V. G. Georguiev, J. P. Vary, W. E. Ormand, A. Nogga, Phys. Rev. Lett. **99**, 024501 (2007).
34. R. Roth, J. Langhammer, A. Calci, S. Binder, P. Navratil, Phys. Rev. Lett. **107**, 072501 (2011).
35. E. Epelbaum, H. Krebs, D. Lee, and U.-G. Meißner, Phys. Rev. Lett. **106**, 192501 (2011).
36. W. R. Zimmerman, M. W. Ahmed, B. Bromberger, S. C. Stave, A. Breskin, V. Dandendorff, T. Delbar and M. Gai *et al.*, Phys. Rev. Lett. **110**, no. 15, 152502 (2013).
37. T. A. Lähde, E. Epelbaum, H. Krebs, D. Lee, U.-G. Meißner and G. Rupak, Phys. Lett. B **732**, 110 (2014).
38. H. Oberhammer, A. Csoto and H. Schlattl, Science **289**, 88 (2000).
39. E. Epelbaum, A. Nogga, W. Gloeckle, H. Kamada, U.-G. Meißner and H. Witala, Phys. Rev. C **66**, 064001 (2002).
40. E. Epelbaum, H. Krebs, D. Lee and U.-G. Meißner, Eur. Phys. J. A **41**, 125 (2009).
41. G. Colangelo, J. Gasser and H. Leutwyler, Phys. Rev. Lett. **86** (2001) 5008.
42. J. C. Berengut, E. Epelbaum, V. V. Flambaum, C. Hanhart, U.-G. Meißner, J. Nebreda, and J. R. Peláez, Phys. Rev. D **87**, 085018 (2013).
43. E. Epelbaum, U.-G. Meißner, W. Gloeckle and C. Elster, Phys. Rev. C **65**, 044001 (2002).
44. H. Mütter, C. A. Engelbrecht and G. E. Brown, Nucl. Phys. A **462**, 701 (1987).
45. S. R. Beane and M. J. Savage, Nucl. Phys. A **713**, 148 (2003).
46. E. Epelbaum, U.-G. Meißner and W. Gloeckle, Nucl. Phys. A **714**, 535 (2003).
47. V. V. Flambaum and R. B. Wiringa, Phys. Rev. C **76**, 054002 (2007).
48. J. Soto and J. Tarrus, Phys. Rev. C **85**, 044001 (2012).
49. T. Yamazaki *et al.* [PACS-CS Collaboration], Phys. Rev. D **81**, 111504 (2010).
50. S. R. Beane, E. Chang, S. D. Cohen, W. Detmold, H. W. Lin, T. C. Luu, K. Orginos and A. Parreno *et al.*, Phys. Rev. D **87**, 034506 (2013).
51. E. Epelbaum, H. Krebs, D. Lee, and U.-G. Meißner, Eur. Phys. J. A **45**, 335 (2010).
52. P. F. Bedaque, T. Luu, and L. Platter, Phys. Rev. C **83**, 045803 (2011).
53. T. Lähde, *private communication*.
54. J. C. Berengut, V. V. Flambaum and V. F. Dmitriev, Phys. Lett. B **683**, 114 (2010).
55. T. Damour and J. F. Donoghue, Phys. Rev. D **78**, 014014 (2008).
56. S. Borsanyi, S. Dürr, Z. Fodor, C. Hoelbling, S. D. Katz, S. Krieg, L. Lellouch and T. Lippert *et al.*, arXiv:1406.4088 [hep-lat].
57. E. Epelbaum, H. Krebs, T. A. Lähde, D. Lee and U.-G. Meißner, Phys. Rev. Lett. **110**, 112502 (2013).
58. E. Epelbaum, H. Krebs, T. A. Lähde, D. Lee and U.-G. Meißner, Eur. Phys. J. A **49**, 82 (2013).
59. M. Livio, D. Hollowell, A. Weiss, and J. W. Truran, Nature **340**, 281 (1989).

-
60. S. Weinberg, "Facing Up" (Harvard University Press, Cambridge, Massachusetts, 2001).
 61. H. Oberhummer, A. Cs ot o, and H. Schlattl, Nucl. Phys. A **689**, 269 (2001).
 62. H. Schlattl, A. Heger, H. Oberhummer, T. Rauscher, and A. Cs ot o, Astrophys. Space Sci. **291**, 27 (2004).
 63. G. Rupak and D. Lee, Phys. Rev. Lett. **111**, 032502 (2013).
 64. M. Pine, D. Lee and G. Rupak, Eur. Phys. J. A **49**, 151 (2013).
 65. L. Ubaldi, Phys. Rev. D **81**, 025011 (2010).

